



# Phosphodiesterase-4 inhibition confers a neuroprotective efficacy against early brain injury following experimental subarachnoid hemorrhage in rats by attenuating neuronal apoptosis through the SIRT1/Akt pathway

Qun Li<sup>a,b,1</sup>, Yucong Peng<sup>a,1</sup>, Linfeng Fan<sup>a</sup>, Hangzhe Xu<sup>a</sup>, Pingyou He<sup>a</sup>, Shenglong Cao<sup>a</sup>, Jianru Li<sup>a</sup>, Ting Chen<sup>a</sup>, Wu Ruan<sup>a</sup>, Gao Chen<sup>a,\*</sup>

<sup>a</sup> Department of Neurosurgery, Second Affiliated Hospital, School of Medicine, Zhejiang University, Jiefang Road 88th, Hangzhou 310016, China

<sup>b</sup> Department of Neurosurgery, First Affiliated Hospital, Wenzhou Medical University, Fuxue Road 2th, Wenzhou 325000, China



## ARTICLE INFO

### Keywords:

Subarachnoid hemorrhage  
Early brain injury  
Phosphodiesterase-4  
Sirtuin1  
Akt  
Apoptosis

## ABSTRACT

Phosphodiesterase-4 (PDE4) plays a fundamental role in a range of central nervous system (CNS) insults, however, the role of PDE4 in early brain injury (EBI) after subarachnoid hemorrhage (SAH) remains unclear. The current study was designed to investigate the role of PDE4 in EBI after SAH and explore the potential mechanism. The SAH model in Sprague-Dawley rat was established by endovascular perforation process. Rats were randomly divided into: sham group, SAH + vehicle group, SAH + rolipram (PDE4 inhibitor) group, SAH + rolipram + sirtinol (SIRT1 inhibitor) group and SAH + rolipram + MK2206 (Akt inhibitor) group. Mortality, SAH grades, neurological function, brain edema, immunofluorescence staining and western blotting were performed. Double fluorescence labeling staining indicated that PDE4 was located predominately in neurons after SAH. Rolipram reduced brain edema, improved neurological function in the rat model of SAH. Moreover, rolipram increased the expression of Sirtuin1 (SIRT1) and up-regulated the phosphorylation of Akt, which was accompanied by the reduction of neuronal apoptosis. Administration of sirtinol inhibited the phosphorylation of Akt. Moreover, all the beneficial effects of rolipram against SAH were abolished by both sirtinol and MK2206. These data indicated that PDE4 inhibition by rolipram protected rats against EBI after SAH via suppressing neuronal apoptosis through the SIRT1/Akt pathway. Rolipram might be an important therapeutic drug for SAH.

## 1. Introduction

Subarachnoid hemorrhage (SAH) is a serious cerebrovascular disease with high rates of mortality and disability [1]. Intense studies have indicated that early brain injury (EBI) is the primary cause of poor outcome after SAH [2]. The exact mechanisms of EBI remain controversial [3]. Among the multiple mechanisms involved, apoptosis has been identified to play an important role in the pathological process of EBI [4]. Growing bodies of studies have demonstrated that suppressing neuronal apoptosis could attenuate EBI and improve the neurological function after SAH [5,6]. Thus, more efforts are needed in order to explore the mechanisms of apoptosis and develop novel therapeutic strategies against neuronal apoptosis to improve the outcome of patients with SAH.

Phosphodiesterase-4 (PDE4) is a high-affinity enzyme that specifically hydrolyzes cAMP [7], which typically acts as the second

messenger and mediates a number of cellular process [8,9]. Previous studies indicated that PDE4 inhibitor rolipram exerts neuroprotective role in a range of central nervous system insults including spinal cord injury [10], ischemic stroke [11], and Alzheimer's disease [12].

In spite of great number of studies have been carried out to define the mechanisms of PDE4 mediated brain injury for years, the underlying mechanisms are not fully understood. Recent study indicated that PDE4 regulates the expression and function of Sirtuin1 (SIRT1) [13]. SIRT1 is a member of (NAD<sup>+</sup>)-dependent protein deacetylases. A growing body of evidence indicates that SIRT1 modulates a variety of cellular functions via deacetylating its target proteins, including p53, FoxO3, IRS-2, and nuclear factor kappaB (NF-κB) [14,15]. Recent studies revealed that SIRT1-overexpression could increase the activity of Akt [16,17]. The activation of SIRT1/Akt signaling exerts neuroprotective effects against ischemic stroke via enhancing angiogenesis and neurogenesis [18,19]. However, the interaction between PDE4

\* Corresponding author.

E-mail address: [d-chengao@zju.edu.cn](mailto:d-chengao@zju.edu.cn) (G. Chen).

<sup>1</sup> These authors contributed equally to this work.

**Table 1**  
Experimental design and number of animals used per group.

Part	Groups	Neuro test	BWC	Western blot	Immune- fluorescence staining	Death	Sum
I	sham	16	6	6	4	0	16
	SAH + vehicle	16	6	6	4	7	23
	SAH + rolipram	16	6	6	4	5	21
II	SAH + vehicle	16	6	6	4	7	23
	SAH + rolipram	16	6	6	4	6	22
	SAH + rolipram + sirtinol	16	6	6	4	8	24
	SAH + rolipram + MK2206	16	6	6	4	7	23

Sprague-Dawley male rats with 300–320 g body weight were used. SAH, subarachnoid hemorrhage; BWC, brain water content; TUNEL staining, Terminal deoxynucleotide transferase deoxyuridine triphosphate (dUTP) nick end labeling staining.

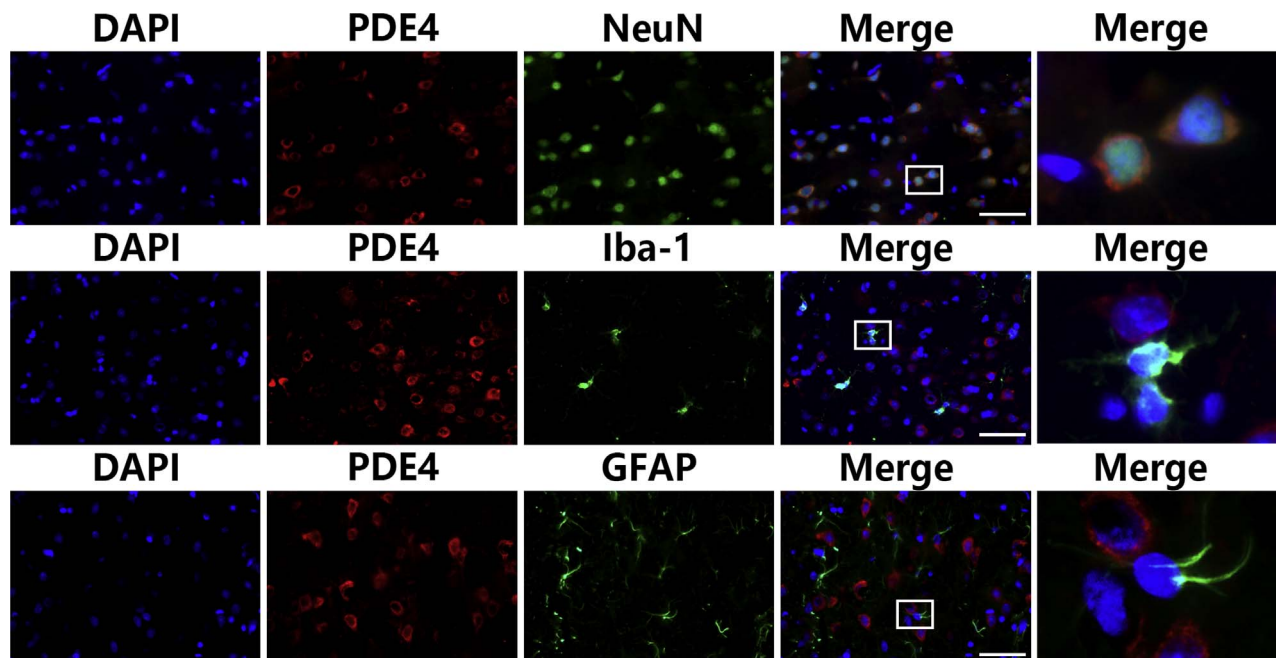


**Fig. 1.** Representative microphotographs of immunofluorescence staining showing localization of PDE4 (red) with NeuN (green), GFAP (green) and Iba-1 (green) in the ipsilateral basal cortex at 24 h after SAH. PDE4 exhibited predominantly neuronal cytoplasmic expression in neurons but not in astrocytes and microglia.  $n = 4$ . Scale bar = 50  $\mu\text{m}$ .

inhibition and the activation of SIRT1/Akt pathway in the pathophysiological process after SAH remains unclearly.

The present study, therefore, was aimed to investigate the role of PDE4 inhibition through rolipram against SAH and explore the potential role of SIRT1/Akt pathway in rolipram mediated neuroprotection.

## 2. Materials and methods

### 2.1. Animals preparation

Adult male Sprague–Dawley (SD) rats weighing 300–320 g were purchased from Slac Laboratory Animal Company Limited (Shanghai, China). The animals were housed at  $25 \pm 1$  °C in a humidity controlled room at the Animal Center of the Second Affiliated Hospital of Zhejiang University with 12 h light/dark cycles. All procedures were approved by the Animal Care Committee of Zhejiang University and were conducted in accordance with the guidelines for the Care and Use of Laboratory Animals of the National Institutes of Health.

### 2.2. Study design

#### 2.2.1. Experiment 1

To determine the neuroprotective effects of PDE4 inhibition against SAH, forty-eight rats (60 rats were used, 12 rats died) were randomly divided into three groups: sham group; SAH + vehicle group; and

SAH + rolipram group ( $n = 16$  for each group). Twenty-four hours after SAH induction, all the parameters were investigated. The neurological score ( $n = 16$ ), SAH grade ( $n = 16$ ), brain water content ( $n = 6$ ), western blot ( $n = 6$ ) and immunofluorescent staining ( $n = 4$ ) were assessed.

#### 2.2.2. Experiment 2

To explore the mechanism of rolipram mediated protection against SAH, sixty-four rats (92 rats were used, 28 died) were divided into four groups: SAH + vehicle group; SAH + rolipram group; SAH + rolipram + sirtinol group and SAH + rolipram + MK2206 group ( $n = 16$  for each group). All the rats were sacrificed at 24 h after SAH. The neurological score ( $n = 16$ ), SAH grade ( $n = 16$ ), brain water content ( $n = 6$ ), western blot ( $n = 6$ ) and immunofluorescent staining ( $n = 4$ ) were performed.

### 2.3. Rat SAH model

The rat SAH was performed using endovascular perforation technique as previously described [20]. Briefly, rats were anesthetized with 40 mg/kg pentobarbital via intraperitoneal injection. Subsequently, the left carotid artery and branches were exposed and dissected. A sharpened 4–0 nylon suture was pushed into the internal carotid artery from the external carotid artery stump until there was resistance. The nylon suture was then advanced 4 mm further to puncture the bifurcation of

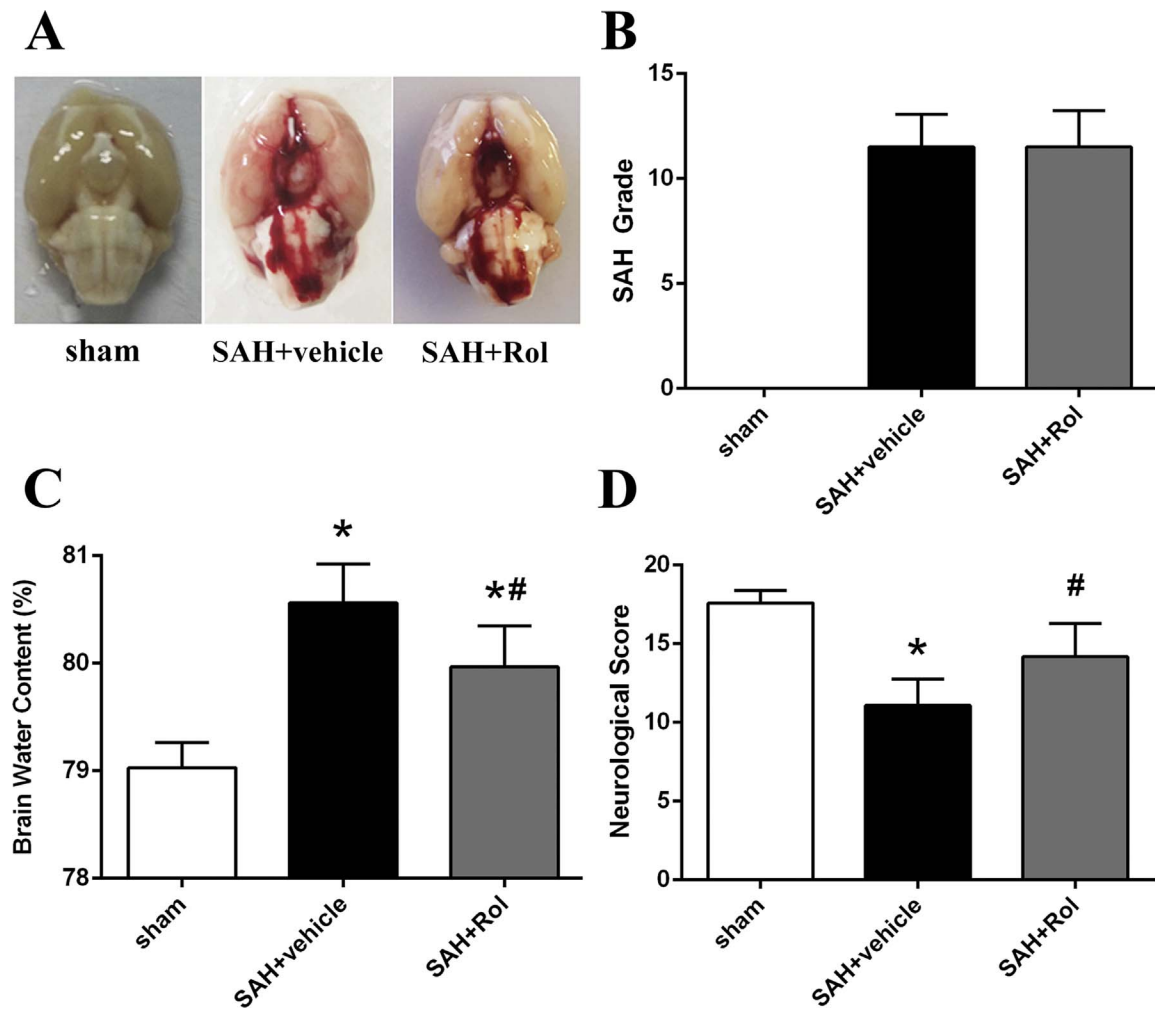


**Fig. 2.** Effects of rolipram on SAH grade, brain water content and neurological score at 24 h after SAH. (A) Typical brains from sham, SAH + vehicle, and SAH + rolipram group. (B) The quantification of SAH severity.  $n = 16$ . (C) The quantification of brain water content.  $n = 6$ . (D) The quantification of neurological score.  $N = 16$ . Data were presented as mean  $\pm$  SD. \* $P < .05$  versus sham group, # $P < .05$  versus SAH + vehicle group.

the middle and anterior cerebral artery. Sham-operated rats underwent the same procedure without perforation.

#### 2.4. Drug administrations

PDE4 inhibitor rolipram (purchased from Selleck Chemicals, Houston, TX) was dissolved in vehicle (0.5% DMSO in 1ml saline) to create a final dosage solutions of 10 mg/kg. Rolipram or vehicle was then injected into peritoneum at two hours after SAH. The dosage and time point of rolipram treatment was based on the previous study [11]. The sham group and SAH + vehicle group received the same volume of sterile saline at the same time points after SAH induction. In experiment 2, the SIRT1 inhibitor sirtinol (purchased from Selleck Chemicals, Houston, TX) was diluted in vehicle (0.5% DMSO) at a concentration of 2 mmol/l and injected into left lateral ventricle 2 h before SAH was induced. The administration of sirtinol was chose according to the previous study [21]. The Akt inhibitor MK2206 (Selleck Chemicals, Houston, TX) was dissolved in DMSO and further diluted in sterile saline to a final DMSO concentration of 0.5%. A total of 5  $\mu$ L MK2206 (100  $\mu$ g) was infused into the left lateral ventricle at a rate of 0.5  $\mu$ L/min 1 h after SAH as previously described [22].

Intracerebroventricular injection was performed as previously described [22]. After the rats were anesthetized with pentobarbital (40 mg/kg) via intraperitoneal injection, a small burr hole was drilled into the skull 1.5 mm posterior and 1.0 mm lateral relative to bregma. A

10  $\mu$ L Hamilton syringe (Microliter701; Hamilton Company, Reno, NV) was used, and the needle was inserted 3.5 mm below the horizontal plane of the bregma into the left lateral ventricle. Then, agent or vehicle was injected to left lateral ventricle. The syringe remained in situ for an additional 10 min before removal.

#### 2.5. SAH grade

The severity of SAH was quantified according to the previously published grading scale [23]. Briefly, the basal cistern was divided into six segments. For each segment, we graded the severity of SAH from 0 to 3 score as follows: Grade 0, no SAH; Grade 1, minimal subarachnoid blood; Grade 2, moderate blood clot with recognizable arteries; and Grade 3, massive hemorrhage covering the cerebral arteries. And the final SAH score was a sum of all six segments. The SAH grade was quantified blindly.

#### 2.6. Neurological score

Neurological score was evaluated with the Garcia Scale System as previously described [24]. Briefly, the evaluation consists of six tests that can be scored 0–3 or 1–3 and include the following: spontaneous activity, symmetry in the movement of four limbs, forepaw outstretching, climbing, body proprioception, and the response to vibrissae touch. Possible scores ranged from 3 to 18. The neurological score was

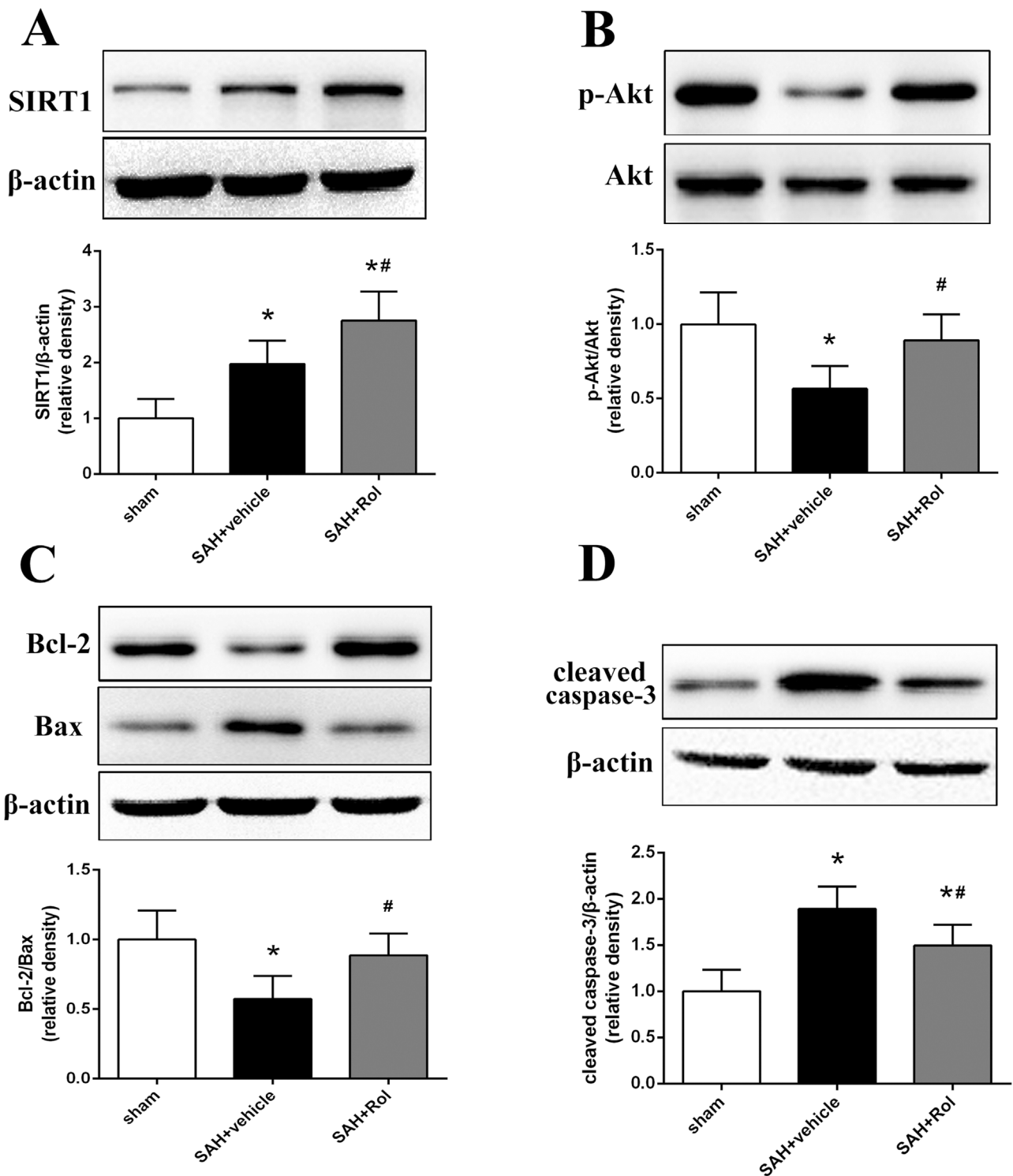


Fig. 3. Effects of rolipram on the phosphorylation of AKT and the expression of SIRT1, Bcl-2, Bax and cleaved caspase-3 after SAH. Rolipram increased the expression of SIRT1 (A), promoted the phosphorylation of Akt (B) and up-regulated the ratio of Bcl-2/Bax (C) while decreased the expression of cleaved caspase-3 (D) at 24 h after SAH. N = 6 for each group. Data were presented as mean  $\pm$  SD. \**P* < .05 versus sham group, #*P* < .05 versus SAH + vehicle group.

evaluated blindly.

### 2.7. Brain water content

Rats were sacrificed under deep anesthesia at 24 h after SAH. The brains were removed and left hemispheres were collected and immediately weighed for the wet weight. And then, the brains were dried in an oven for 24 h at 105 °C to measure the dry weight. The brain water

content was calculated as: (wet weight-dry weight)/wet weight\*100%.

### 2.8. Western blot

Western blot was performed as previously described [6]. Briefly, rats were sacrificed and the left hemispheres were harvested at 24 h after SAH. The protein concentration was measured by using the DC protein assay kit (Bio-Rad). Equal amounts of sample (40  $\mu$ g) were

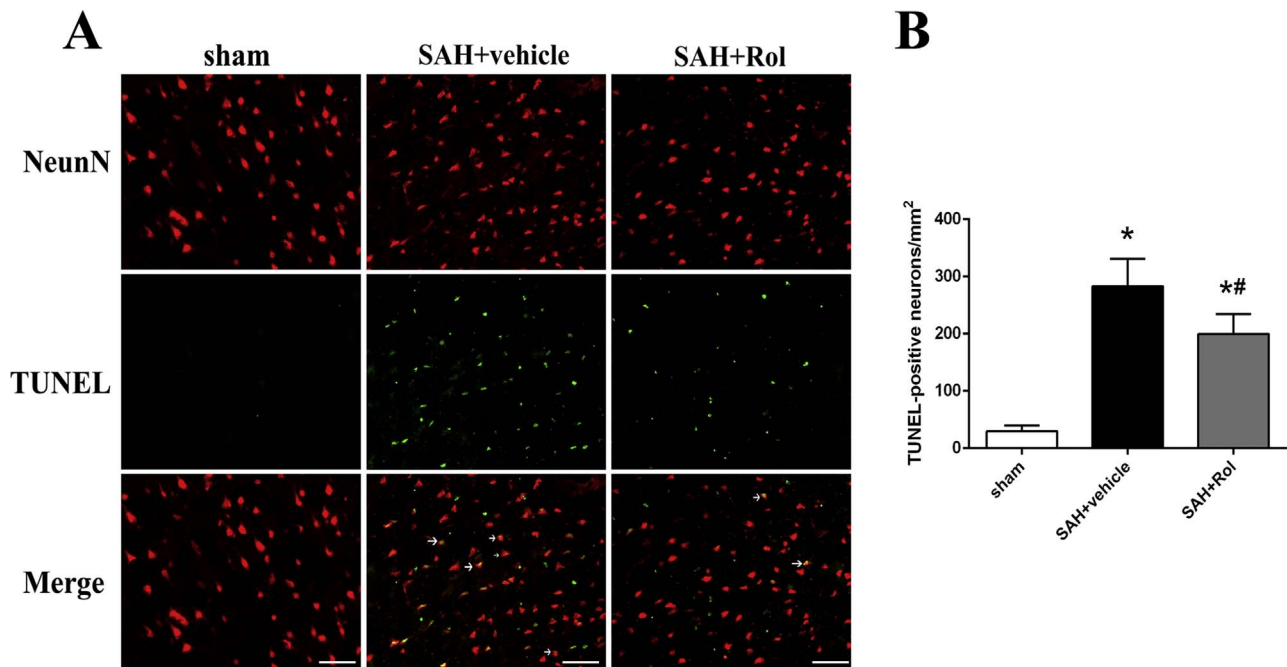


Fig. 4. Rolipram attenuated neuronal apoptosis in ipsilateral cortex after SAH. (A) Representative transferase-mediated deoxyuridine triphosphate-biotin nick end labeling (TUNEL)/NeuN photomicrographs of the ipsilateral cortex in different groups (scale bar = 50  $\mu$ m). Fluorescence colors: DAPI, blue; TUNEL, green; and NeuN, red. (B) Quantification of the TUNEL/NeuN positive cells in the ipsilateral cortex in different groups.  $n = 4$ . Data were presented as mean  $\pm$  SD. \* $P < .05$  versus sham group; # $P < .05$  versus SAH + vehicle group.

loaded into sodium dodecyl sulfate–polyacrylamide gels and electrophoresed at 100 V for 1 h. And then, proteins were transferred onto polyvinylidene fluoride membranes. The membranes were blocked with fat-free milk buffer for 2 h and then incubated overnight at 4 °C with primary antibodies against SIRT1 (#ab-110304, 1:1000; Abcam), p-Akt (cst#9275, 1:1000; Cell Signaling Technology), Akt (cst#9272S, 1:1000; Cell Signaling Technology), Bax (#ab-32503, 1:1000; Abcam), Bcl-2(#ab-59348, 1:1000; Abcam), cleaved caspase-3 (#ab-14607, 1:1000; Abcam), ac-NF- $\kappa$ B (cst#12629S, 1:500, Cell Signaling), and  $\beta$ -actin (#ab-8226, 1:1000; Abcam). The membranes were processed with horseradish peroxidase-conjugated secondary antibodies at room temperature for 1 h. Bands were visualized using the ECL Plus chemiluminescence reagent kit (Amersham Bioscience, Arlington Heights, IL). The band densities were quantified with the Image J software (National Institutes of Health, Bethesda, MD, USA). To facilitate comparison between the groups, the band density values were normalized to the mean value of the control group.

## 2.9. Immunofluorescence staining and quantification of neuronal apoptosis

Rats were anesthetized and perfused with 0.1M PBS followed by 4% paraformaldehyde (pH 7.4). Brains were harvested and soaked in 4% PFA at 4 °C for 24 h. Subsequently, brains were transferred into a 30% sucrose solution for 2 days. Coronal frozen sections (8  $\mu$ m) were placed onto slides for fluorescence staining. The brain sections were pre-processed for 60 min in 0.01 mmol PBS (pH, 7.4) containing 10% normal serum consistent with secondary antibody and 0.3% Triton X-100. Then, the brain sections were incubated overnight at 4 °C with primary antibodies: rabbit anti-PDE4 (#ab-14628, 1:500; Abcam), mouse anti-NeuN (#ab-104224, 1:500; Abcam), mouse anti-GFAP (#ab-7260, 1:500; Abcam), and goat anti-Iba-1 (#ab-5076, 1:500; Abcam). Sections were then washed with 0.01 M PBS and incubated for 2 h at room temperature with secondary antibodies. Terminal deoxynucleotide transferase deoxyuridine triphosphate (dUTP) nick end labeling (TUNEL) staining was performed to detect the death of cells according to the manufacturer's protocol (Roche Inc., Basel, Switzerland). The extent of neuronal damage was evaluated by an

apoptotic index, which was calculated as the average number of TUNEL-positive neurons in six sections per brain. The data were expressed as cells per square millimeter. The sections were visualized by a fluorescence microscope. Photomicrographs were saved and merged with Image Pro Plus software (Olympus, Melville, NY).

## 2.10. Statistical analysis

All statistical analyses were performed using GraphPad Prism 6 (GraphPad Software Inc., San Diego, CA, USA). Data are presented as mean  $\pm$  standard deviation (SD). Statistical significance was analyzed by a one-way analysis of variance (ANOVA) followed by Turkey test for multiple comparisons. Statistical significance was inferred at  $P < .05$ .

## 3. Results

### 3.1. Physiological data and mortality

The mean arterial pressure (85–125 mm Hg), arterial pH (7.35–7.45), PO<sub>2</sub> (80–95 mm Hg), PCO<sub>2</sub> (35–45 mm Hg), and blood glucose levels (95–125 mg/dL) were monitored during the surgical procedure. And no significant changes in these physiological variables were noted among different groups.

None of the animals died in the sham group. In the first experiment, the mortality rate was 30.4% (7 of 23) in the SAH + vehicle group; and 23.8% (5 of 21) in the SAH + rolipram group. In the second experiment, the mortality rate at 24 h after SAH was 30.4% (7 of 23) in the SAH + vehicle group, 27.3% (6 of 22) in the SAH + rolipram group, 33.3% (8 of 24) in the SAH + rolipram + sirtinol group, 30.4% (7 of 23) in the SAH + rolipram + MK2206 group (Table 1).

### 3.2. The distribution of PDE4 in left hemisphere after SAH

The distribution of PDE4 was identified by double immunofluorescence staining. As shown (Fig. 1), PDE4 was mainly located in neurons rather than microglia or astrocytes at 24 h after SAH in the ipsilateral cortex.

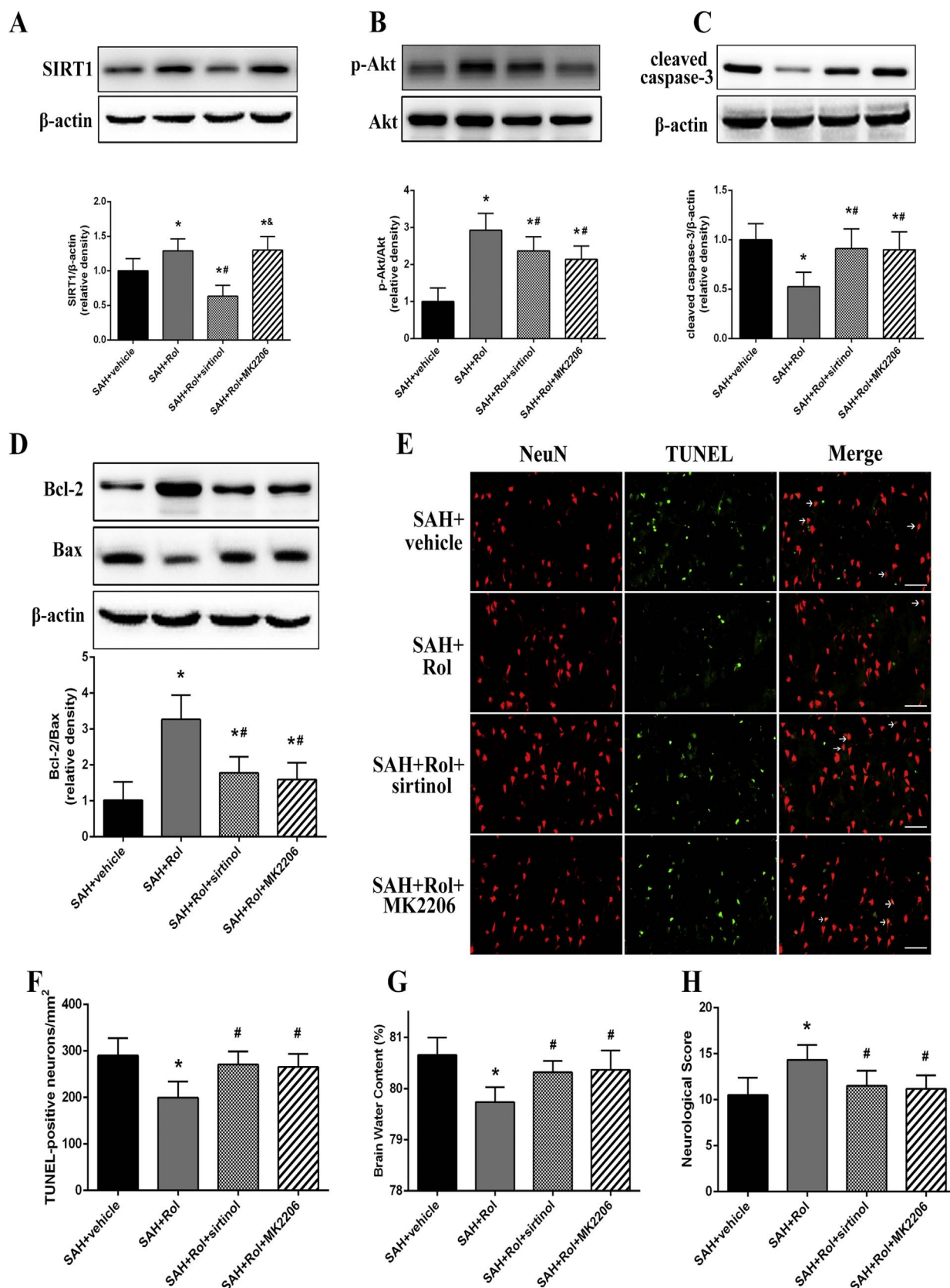


**Fig. 5.** Role of SIRT1/Akt pathway in rolipram-mediated neuroprotection against SAH. (A–B) Sirtinol decreased the expression of SIRT1 and inhibited the phosphorylation of Akt. And MK2206 inhibited the phosphorylation of Akt, while the expression of SIRT1 was not affected. Rolipram treatment increased ratio of Bcl-2/Bax as well as reduced Bax, cleaved caspase-3 expression and restrict the neuronal apoptosis; however, these protective effects were reversed by both sirtinol and MK2206 (C, D E and F). Both sirtinol and MK2206 abolish the beneficial effects induced by rolipram in attenuating brain edema (G) and alleviating neurological dysfunction (H). N = 6 for western blot, n = 4 for immunofluorescence. Scale bar = 50 μm. n = 6 for quantification of brain water content. And n = 16 for quantification of neurological score. Data were presented as mean ± SD. \*P < .05 versus sham group, #P < .05 versus SAH + vehicle group.

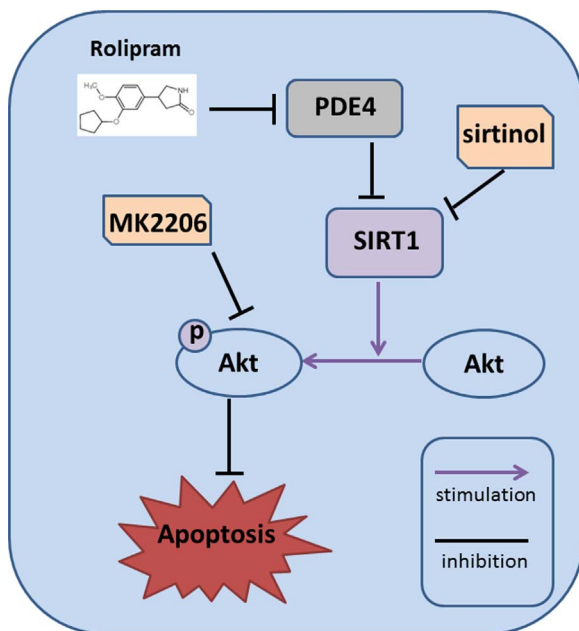


Fig. 6. Schematic diagram shows potential molecular mechanisms of rolipram induced neuroprotection against SAH.

### 3.3. PDE4 inhibition through rolipram attenuated brain edema and neurological dysfunction after SAH

Brain edema and neurobehavioral function were evaluated blindly at 24 h after SAH. Representative brains from the sham group and SAH groups were presented in Fig. 2A. The blood clots were mainly located around the circle of Willis and brainstem. The SAH score of sham group was zero, and no significant difference on SAH score was observed between the SAH groups (Fig. 2B). Brain water content was measured to evaluate the severity of brain edema at 24 h after SAH. Brain water content was significantly increased after SAH ( $P < .05$  versus sham group, Fig. 2C), which was remarkably reduced by rolipram ( $P < .05$  versus SAH + vehicle, Fig. 2C).

Accordingly, neurological score was remarkably decreased after SAH when compared with sham group ( $P < .05$ , Fig. 2D), and administration of rolipram significantly ameliorated the neurological deficits ( $P < .05$  versus SAH + vehicle, Fig. 2D).

### 3.4. Rolipram increased the expression of SIRT1 and up-regulated the phosphorylation of Akt after SAH

The expression of SIRT1 was increased in the ipsilateral cortex after SAH ( $P < .05$  versus sham, Fig. 3A). And compared with SAH + vehicle group, administration of rolipram significantly up-regulated the expression of SIRT1 ( $P < .05$ , Fig. 3A). The phosphorylation of Akt decreased after SAH ( $P < .05$  versus sham, Fig. 4B). And rolipram significantly promoted the phosphorylation of Akt at 24 h after SAH ( $P < .05$  versus SAH + vehicle, Fig. 4B).

### 3.5. Rolipram attenuated neuronal apoptosis after SAH

Given that rolipram influence the expression of SIRT1 and Akt, both of which regulate apoptosis under pathophysiological conditions [18], western blot was performed to assess the expression of apoptosis related biomarkers after SAH. The ratio of Bcl-2/Bax was remarkably decreased, while the expression of cleaved caspase-3 significantly elevated after SAH ( $P < .05$  versus sham, Fig. 3). However, administration of rolipram remarkably reversed these changes ( $P < .05$  versus SAH + vehicle group, Fig. 3).

TUNEL/NeuN immunofluorescent double-labeling was conducted to

further demonstrate the neuronal apoptosis. The total number of TUNEL-positive neurons was significantly increased in after SAH ( $P < .05$  versus sham, Fig. 4). And treatment with rolipram remarkably reduced the number of TUNEL-positive neurons ( $P < .05$  versus SAH + vehicle group, Fig. 4).

### 3.6. Role of SIRT1/Akt pathway in rolipram mediated neuroprotection against SAH

Given that PDE4 inhibition by rolipram activated both SIRT1 and Akt (As shown in Fig. 3), the specific SIRT1 inhibitor sirtinol, and selective Akt inhibitor MK2206 were used to further verify the potential neuroprotective mechanism of rolipram against SAH. As shown in Fig. 5, rolipram remarkably increased the expression of SIRT1 and phosphorylation of Akt ( $P < .05$  versus SAH + vehicle, Fig. 5), which were significantly reversed by sirtinol ( $P < .05$  versus SAH + rolipram, Fig. 5). Moreover, administration of MK2206 remarkably inhibited the phosphorylation of Akt ( $P < .05$  versus SAH + rolipram, Fig. 5), while the expression of SIRT1 was not affected ( $P > .05$  versus SAH + rolipram, Fig. 5).

In addition, both sirtinol and MK2206 significantly increased the number of TUNEL-positive neuron as well as the up-regulated the expression of cleaved caspase-3, while decreased the ratio of Bcl-2/Bax. ( $P < .05$  versus SAH + rolipram, Fig. 5). More importantly, the neuroprotective effects of rolipram on decreasing brain water content and improving neurological score were significantly reversed by sirtinol and MK2206 ( $P < .05$  versus SAH + vehicle group, Fig. 5G, H).

## 4. Discussion

In the current study, we investigated the role of rolipram, a specific inhibitor of PDE4, in early brain injury after SAH and explore the potential mechanisms. We made the major observations as follows: (1) PDE4 was located mainly in neurons at 24 h after SAH; (2) PDE4 inhibition by rolipram alleviated brain edema and neurological deficits after SAH; (3) rolipram exert protective effects against SAH via reducing neuronal apoptosis; (4) SIRT1 promoted the phosphorylation and activation of Akt after SAH; (5) the neuroprotective effects of rolipram against EBI following SAH is associated with the SIRT1/Akt signaling. These data indicate that PDE4 inhibition might be an important therapeutic strategy for SAH treatment (Fig. 6).

PDE4 is a high-affinity enzyme consists with four variants (PDE4A-D), both of which can specifically hydrolyze cAMP and subsequently influence the cell process such as DNA repair, cellular differentiation and survival [7]. The protective effects of PDE4 inhibition in attenuating tissue injury such as acute kidney injury, heart failure and asthma, has been studied for decades [25–27]. More importantly, recent studies has detected that PDE4 participates in the pathophysiological process of several central nervous system disorders such as ischemia stroke, experimental allergic encephalomyelitis (EAE) and Alzheimer's disease [28–30]. In spite of the neuroprotective capacity of PDE4 inhibition by rolipram has been studied for years, the role of PDE4 in EBI following SAH remains unknown.

Therefore, in the first part of the present study, we determine the location of PDE4 on brain by double-immunofluorescence staining. Our result indicated that PDE4 was mainly expressed on neurons at 24 h after SAH, which suggested that PDE4 might play a critical role in determining the survival of neurons.

Base on the evidence mentioned above, we further investigated the role of PDE4 in EBI after SAH. Rolipram, the specific inhibitor of PDE4 which typically acts as an antidepressant agent, is one of the most widely used compound to investigate the role of PDE4 on central nerve system since its property that readily crosses blood-brain barrier and concentrate in brain tissue [28]. Our results indicated that rolipram significantly alleviated brain edema and attenuated neurological dysfunction after SAH. A growing number of studies indicated that

apoptosis, which is characterized by distinctive morphologic changes, cell shrinkage, nuclear fragmentation, chromatin condensation, and chromosomal DNA fragmentation, plays a critical role in the pathophysiological process of EBI after SAH [3]. Therefore, in the next part of the present study, we investigated the effect of rolipram in regulating neuronal apoptosis after SAH. And consistent with previous studies including ours, the apoptotic neurons significantly increased after SAH [6,21]. The expression of cleaved caspase-3 and the number of TUNEL-positive neuron increased, while the ratio of Bcl-2/Bax decreased at 24 h after SAH. However, treated rats with rolipram remarkably reversed these changes. Rolipram rescued rats against SAH though alleviating apoptosis.

In the rest part of the present study, we explored the potential mechanism of rolipram mediated anti-apoptotic effect against SAH. Recent study demonstrated that rolipram up-regulates the expression and activity of SIRT1 [13]. Rolipram elevated cAMP levels and subsequently activated the cAMP effector protein Epac1. The activation of Epac1 increases intracellular Ca(2+) levels and induces the activation of CamKK $\beta$ -AMPK pathway through phospholipase C and the ryanodine receptor Ca(2+)-release channel. And ultimately increases NAD(+) and the function of SIRT1. SIRT1 is a nicotinamide (NAD+)-dependent deacetylases that widely expressed in central nervous system. Once activated, SIRT1 deacetylases the downstream substrates such as FoxO3, NF- $\kappa$ B, proliferator-activated receptor-gamma (PPAR $\gamma$ ) and PPAR $\gamma$  coactivator-1 $\alpha$  (PGC-1 $\alpha$ ), and subsequently regulates various cellular processes [31,32]. In spite of the beneficial effects of SIRT1 in the central nervous system has been studied for years [21,33–35], the underlying mechanisms of SIRT1 induced neuroprotection against EBI after SAH are not fully understood.

Akt, also known as protein kinase B, is a serine-threonine kinase which can be activated by PI3K products in the phosphorylated form (p-Akt). There are three AKT isoforms (AKT1, 2 and 3), each of the isoform shares three highly conserved domains: catalytic domain, hydrophobic motif and pleckstrin homology (PH) domain [36]. PH domain contains a lipid-binding module that promotes the localization of AKT to the plasma membrane, an important step in Akt activation [37]. The movement of AKT from cytoplasm to the plasma membrane induces the activation of the kinase by phosphorylation on Thr308 in the activation loop and Ser473 in the hydrophobic motif, and regulates the phosphorylation of Akt substrates, such as PRAS40, TSC2 and GSK3 $\beta$ , and ultimately modulates a variety of physiological and pathophysiological processes [36,38]. Recent studies have indicated interaction between SIRT1 and the activation of Akt. Briefly, histone acetyltransferases EP300 and KAT2B acetylate Akt on Lys-14 and Lys-20. The acetylation of Akt results in reduced phosphorylation and inhibition of Akt activity. However, the histone deacetylase SIRT1 deacetylates Akt on both Lys-14 and Lys-20, and subsequently results in relieving the inhibition and promoting the activation of Akt [16,17].

Given that both SIRT1 and Akt exert important role on neuronal survival [21,39] and rolipram could increase the SIRT1 signaling, we tried to identify the role of SIRT1 and Akt signaling on rolipram mediated-neuroprotective effects against SAH. Our data indicated that rolipram treatment significantly increased the expression of SIRT1 and up-regulated the phosphorylation of Akt, which was paralleled with its neuroprotective effects by suppressing neuronal apoptosis after SAH. In addition, administration of sirtinol, the SIRT1 inhibitor, decreased the phosphorylation of Akt. And the Akt inhibitor MK2206 significantly inhibited the phosphorylation of Akt, while the expression of SIRT1 was not affected. These results suggested that Akt might be the downstream target and modulated by SIRT1, which was consistent with previous study [16,17]. Furthermore, both sirtinol and MK2206 reserved the neuroprotective effects of rolipram in alleviating brain edema and neurological impairment as well as reducing neuronal apoptosis.

There are several limitations in our study. Firstly, several studies have revealed the role of rolipram in regulating neuroinflammation [11]. In the present study, we focused on anti-apoptosis effect of

rolipram after SAH. Therefore, further studies are required to explore the role of PDE4 inhibition on neuroinflammation after SAH. Secondly, given that the half-life of rolipram is short (1–3 h) [28], further studies are warranted to identify the optimum dosage, time point and application routes of rolipram to better study the role of PDE4 on the pathophysiological process of SAH. Thirdly, several studies demonstrated that rolipram is beneficial for CNS disease in long-term treatment [12], and in present study, we focused on the neuroprotective effects of PDE4 inhibition on EBI after SAH, thus, further studies focused on the long-term neuroprotective effects of rolipram in SAH might be required. Finally, in the present study, our data indicated that SIRT1 could promote the phosphorylation and activation of Akt. However, the exact mechanism remains unclearly. Therefore, further efforts might be required to reveal the exact mechanism of the interaction between SIRT1 and Akt activation under SAH condition in the further.

## 5. Conclusion

The experimental data suggest that PDE4 plays an important role in the pathophysiological process of EBI after SAH. And inhibition PDE4 by rolipram has the potential to attenuate EBI following SAH via suppressing neuronal apoptosis through the SIRT1/Akt pathway. Rolipram could be a novel and promising therapeutic drug for SAH.

## Conflict of interest

The authors declare that they have no conflict of interest.

## Acknowledgment

This work was supported by the National Natural Science Foundation of China (No. 81571106).

## Appendix A. Supplementary data

Supplementary material related to this article can be found, in the online version, at doi:<https://doi.org/10.1016/j.biopha.2018.01.093>.

## References

- [1] K.J. Becker, Epidemiology and clinical presentation of aneurysmal subarachnoid hemorrhage, *Neurosurg. Clin. N. Am.* 9 (3) (1998) 435–444.
- [2] F.A. Sehba, J. Hou, R.M. Pluta, J.H. Zhang, The importance of early brain injury after subarachnoid hemorrhage, *Prog. Neurobiol.* 97 (1) (2012) 14–37.
- [3] S. Chen, H. Feng, P. Sherchan, D. Klebe, G. Zhao, X. Sun, J. Zhang, J. Tang, J.H. Zhang, Controversies and evolving new mechanisms in subarachnoid hemorrhage, *Prog. Neurobiol.* 115 (2014) 64–91.
- [4] Y. Hasegawa, H. Suzuki, T. Sozen, O. Altay, J.H. Zhang, Apoptotic mechanisms for neuronal cells in early brain injury after subarachnoid hemorrhage, *Acta. Neurochir. Suppl.* 110 (Pt 1) (2011) 43–48.
- [5] L. Zhao, R. An, Y. Yang, X. Yang, H. Liu, L. Yue, X. Li, Y. Lin, R.J. Reiter, Y. Qu, Melatonin alleviates brain injury in mice subjected to cecal ligation and puncture via attenuating inflammation, apoptosis, and oxidative stress: the role of SIRT1 signaling, *J. Pineal Res.* 59 (2) (2015) 230–239.
- [6] J. Chen, L. Wang, C. Wu, Q. Hu, C. Gu, F. Yan, J. Li, W. Yan, G. Chen, Melatonin-enhanced autophagy protects against neural apoptosis via a mitochondrial pathway in early brain injury following a subarachnoid hemorrhage, *J. Pineal Res.* 56 (1) (2014) 12–19.
- [7] H.J. Dyke, J.G. Montana, Update on the therapeutic potential of PDE4 inhibitors, *Expert Opin. Invest. Drugs* 11 (1) (2002) 1–13.
- [8] B.S. Skalhegg, K. Tasken, Specificity in the cAMP/PKA signaling pathway. differential expression, regulation, and subcellular localization of subunits of PKA, *Front. Biosci.* 5 (2000) D678–D693.
- [9] C.A. Barlow, K. Kitiphongspattana, N. Siddiqui, M.W. Roe, B.T. Mossman, K.M. Lounsbury, Protein kinase A-mediated CREB phosphorylation is an oxidant-induced survival pathway in alveolar type II cells, *Apoptosis* 13 (5) (2008) 681–692.
- [10] E. Nikulina, J.L. Tidwell, H.N. Dai, B.S. Bregman, M.T. Filbin, The phosphodiesterase inhibitor rolipram delivered after a spinal cord lesion promotes axonal regeneration and functional recovery, *Proc. Natl. Acad. Sci. U. S. A.* 101 (23) (2004) 8786–87890.
- [11] P. Kraft, T. Schwarz, E. Gob, N. Heydenreich, M. Brede, S.G. Meuth, C. Kleinschnitz,

- The phosphodiesterase-4 inhibitor rolipram protects from ischemic stroke in mice by reducing blood-brain-barrier damage, inflammation and thrombosis, *Exp. Neurol.* 247 (2013) 80–90.
- [12] C. Wang, X.M. Yang, Y.Y. Zhuo, H. Zhou, H.B. Lin, Y.F. Cheng, J.P. Xu, H.T. Zhang, The phosphodiesterase-4 inhibitor rolipram reverses Abeta-induced cognitive impairment and neuroinflammatory and apoptotic responses in rats, *Int. J. Neuropsychopharmacol.* 15 (6) (2012) 749–766.
- [13] S.J. Park, F. Ahmad, A. Philp, K. Baar, T. Williams, H. Luo, H. Ke, H. Rehmann, R. Taussig, A.L. Brown, M.K. Kim, M.A. Beaven, A.B. Burgin, V. Manganiello, J.H. Chung, Resveratrol ameliorates aging-related metabolic phenotypes by inhibiting cAMP phosphodiesterases, *Cell* 148 (3) (2012) 421–433.
- [14] P. Singh, P.S. Hanson, C.M. Morris, SIRT1 ameliorates oxidative stress induced neural cell death and is down-regulated in Parkinson's disease, *BMC Neurosci.* 18 (1) (2017) 46.
- [15] S. Chung, H. Yao, S. Caito, J.W. Hwang, G. Arunachalam, I. Rahman, Regulation of SIRT1 in cellular functions: role of polyphenols, *Arch Biochem. Biophys.* 501 (1) (2010) 79–90.
- [16] N.R. Sundaresan, V.B. Pillai, D. Wolfgeher, S. Samant, P. Vasudevan, V. Parekh, H. Raghuraman, J.M. Cunningham, M. Gupta, M.P. Gupta, The deacetylase SIRT1 promotes membrane localization and activation of Akt and PDK1 during tumorigenesis and cardiac hypertrophy, *Sci. Signal.* 4 (182) (2011) ra46.
- [17] J. Iaconelli, J. Lalonde, B. Watmuff, B. Liu, R. Mazitschek, S.J. Haggarty, R. Karmacharya, Lysine deacetylation by HDAC6 regulates the kinase activity of AKT in human neural progenitor cells, *ACS Chem. Biol.* 12 (8) (2017) 2139–2148.
- [18] J. Shin, K. Lee, H. Kim, E. Park, Acute resveratrol treatment modulates multiple signaling pathways in the ischemic brain, *Neurochem. Res.* 37 (12) (2012) 2686–2696.
- [19] D. Hermann, A. Zechariah, B. Kaltwasser, B. Bosche, A. Caglayan, E. Kilic, T. Doepfner, Sustained neurological recovery induced by resveratrol is associated with angiogenesis rather than neuroprotection after focal cerebral ischemia, *Neurobiol. Dis.* 83 (2015) 16–25.
- [20] J. Wu, Y. Zhang, P. Yang, B. Enkhjargal, A. Manaenko, J. Tang, W.J. Pearce, R. Hartman, A. Obenaus, G. Chen, J.H. Zhang, Recombinant osteopontin stabilizes smooth muscle cell phenotype via integrin receptor/integrin-linked Kinase/Rac-1 pathway after subarachnoid hemorrhage in rats, *Stroke* 47 (5) (2016) 1319–1327.
- [21] X.S. Zhang, Q. Wu, L.Y. Wu, Z.N. Ye, T.W. Jiang, W. Li, Z. Zhuang, M.L. Zhou, X. Zhang, C.H. Hang, Sirtuin 1 activation protects against early brain injury after experimental subarachnoid hemorrhage in rats, *Cell. Death Dis.* 7 (10) (2016) e2416.
- [22] F. Yan, S. Cao, J. Li, B. Dixon, X. Yu, J. Chen, C. Gu, W. Lin, G. Chen, Pharmacological inhibition of PERK attenuates early brain injury after subarachnoid hemorrhage in rats through the activation of Akt, *Mol. Neurobiol.* 54 (3) (2017) 1808–1817.
- [23] T. Sugawara, R. Ayer, V. Jadhav, J.H. Zhang, A new grading system evaluating bleeding scale in filament perforation subarachnoid hemorrhage rat model, *J. Neurosci. Methods* 167 (2) (2008) 327–334.
- [24] J.H. Garcia, S. Wagner, K.F. Liu, X.J. Hu, Neurological deficit and extent of neuronal necrosis attributable to middle cerebral artery occlusion in rats, *Stat. Validation Stroke* 26 (4) (1995) 627–634 Discussion 635.
- [25] S. Beca, P.B. Helli, J.A. Simpson, D. Zhao, G.P. Farman, P. Jones, X. Tian, L.S. Wilson, F. Ahmad, S.R.W. Chen, M.A. Movsesian, V. Manganiello, D.H. Maurice, M. Conti, P.H. Backx, Phosphodiesterase 4D regulates baseline sarcoplasmic reticulum Ca<sup>2+</sup> release and cardiac contractility, independently of L-type Ca<sup>2+</sup> current, *Circ. Res.* 109 (9) (2011) 1024–1030.
- [26] L.E. Kistemaker, T.A. Oenema, H.A. Baarsma, I.S.T. Bos, M. Schmidt, F. Facchinetti, M. Civelli, G. Villetti, R. Gosens, The PDE4 inhibitor CHF-6001 and LAMAs inhibit bronchoconstriction-induced remodelling in lung slices, *Am. J. Physiol Lung Cell. Mol. Physiol.* 313 (2017), <http://dx.doi.org/10.1152/ajplung.00069.2017>.
- [27] C.R. Sims, S.P. Singh, S. Mu, N. Gokden, D. Zakaria, T.C. Nguyen, P.R. Mayeux, Rolipram improves outcome in a rat model of infant sepsis-induced cardiorenal syndrome, *Front. Pharmacol.* 8 (2017) 237.
- [28] W. Krause, G. Kuhne, Pharmacokinetics of rolipram in the rhesus and cynomolgus monkeys, the rat and the rabbit, *Stud. Species Differences Xenobiotica* 18 (5) (1988) 561–571.
- [29] C.S. Moore, N. Earl, R. Frenette, A. Styhler, J.A. Mancini, D.W. Nicholson, A.L. Hebb, T. Owens, G.S. Robertson, Peripheral phosphodiesterase 4 inhibition produced by 4-[2-(3,4-Bis-difluoromethoxyphenyl)-2-[4-(1,1,1,3,3,3-hexafluoro-2-hydroxypropan-2-yl)-phenyl]-ethyl]-3-methylpyridine-1-oxide (L-826,141) prevents experimental autoimmune encephalomyelitis, *J. Pharmacol. Exp. Ther.* 319 (1) (2006) 63–72.
- [30] M.E. Gurney, E.C. D'Amato, A.B. Burgin, Phosphodiesterase-4 (PDE4) molecular pharmacology and Alzheimer's disease, *Neurotherapeutics* 12 (1) (2015) 49–56.
- [31] A.Z. Herskovits, L. Guarente, SIRT1 in neurodevelopment and brain senescence, *Neuron* 81 (3) (2014) 471–483.
- [32] J.W. Hwang, H. Yao, S. Caito, I.K. Sundar, I. Rahman, Redox regulation of SIRT1 in inflammation and cellular senescence, *Free. Radic. Biol. Med.* 61 (2013) 95–110.
- [33] K.B. Koronowski, M.A. Perez-Pinzon, Sirt1 in cerebral ischemia, *Brain Circ.* 1 (1) (2015) 69–78.
- [34] J. Gao, R. Zhou, X. You, F. Luo, H. He, X. Chang, L. Zhu, X. Ding, T. Yan, Salidroside suppresses inflammation in a D-galactose-induced rat model of Alzheimer's disease via SIRT1/NF-kappaB pathway, *Metab. Brain Dis.* 31 (4) (2016) 771–778.
- [35] H. Chen, H. Ji, M. Zhang, Z. Liu, L. Lao, C. Deng, J. Chen, G. Zhong, An agonist of the protective factor SIRT1 improves functional recovery and promotes neuronal survival by attenuating inflammation after spinal cord injury, *J. Neurosci.* (2017).
- [36] V. Calleja, M. Laguerre, P.J. Parker, B. Larjani, Role of a novel PH-kinase domain interface in PKB/Akt regulation: structural mechanism for allosteric inhibition, *PLoS Biol.* 7 (1) (2009) e17.
- [37] J.S. Brown, U. Banerji, Maximising the potential of AKT inhibitors as anti-cancer treatments, *Pharmacol. Ther.* 172 (2017) 101–115.
- [38] T.A. Yap, L. Yan, A. Patnaik, I. Fearon, D. Olmos, K. Papadopoulos, R.D. Baird, L. Delgado, A. Taylor, L. Lupinacci, R. Riisnaes, L.L. Pope, S.P. Heaton, G. Thomas, M.D. Garrett, D.M. Sullivan, J.S. de Bono, A.W. Tolcher, First-in-man clinical trial of the oral pan-AKT inhibitor MK-2206 in patients with advanced solid tumors, *J. Clin. Oncol.* 29 (35) (2011) 4688–4695.
- [39] Y. Dai, W. Zhang, X. Zhou, J. Shi, Activation of the protein Kinase B (Akt) reduces Nur77-induced apoptosis during early brain injury after experimental subarachnoid hemorrhage in rat, *Ann. Clin. Lab Sci.* 45 (6) (2015) 615–622.